



## Limitation in Fabricating PSf/ZIF-8 Hollow Fiber Membrane for CO<sub>2</sub>/CH<sub>4</sub> Separation

Nik Abdul Hadi Md Nordin <sup>1\*</sup>, Ahmad Fauzi Ismail <sup>2</sup>, Surya Murali Racha <sup>2</sup>, Ng Be Cheer <sup>2</sup>, Muhammad Roil Bilad <sup>1</sup>, Zulfan Adi Putra <sup>1</sup>, Mohd Dzul Hakim Wirzal <sup>1</sup>

<sup>1</sup> Chemical Engineering Department, Universiti Teknologi PETRONAS (UTP), 32610 Seri Iskandar, Perak, Malaysia

<sup>2</sup> Advanced Membrane Technology Research Centre (AMTEC), Universiti Teknologi Malaysia (UTM), 81310 Skudai, Johor, Malaysia

Correspondence: E-mail: [nahadi.sapiaa@utp.edu.my](mailto:nahadi.sapiaa@utp.edu.my)

### ABSTRACTS

Hollow fiber membrane configuration is way forward in membrane development since it possesses higher packing density and effective surface area per unit module compared to other configuration. Since majority of mixed matrix membrane (MMM) for gas separation reported focuses on flat sheet membrane development, this report aims to address the challenges faced in fabricating hollow fiber MMM. In this study, hollow fiber formulation is fabricated and their MMM using different types of fillers (virgin and modified ZIF-8) are prepared and used as a dispersed phase. The neat hollow fiber membrane shows good results with CO<sub>2</sub> permeance of 104.39 GPU and CO<sub>2</sub>/CH<sub>4</sub> selectivity of 29.28, in comparison with reported literature. Upon filler incorporation, the resulted MMMs appear to be diminished in both CO<sub>2</sub> permeance and CO<sub>2</sub>/CH<sub>4</sub> selectivity. While using modified ZIF-8, lesser deterioration was shown compared to pure ZIF-8, this phenomenon is likely to occur due to the changes in solution stability which causes notable changes in membrane morphology and performances.

© 2018 Tim Pengembang Jurnal UPI

### ARTICLE INFO

#### Article History:

Received 16 Aug 2018

Revised 20 Aug 2018

Accepted 25 Aug 2018

Available online 09 Sep 2018

#### Keywords:

Hollow fiber membrane, mixed matrix membrane, metal-organic framework, zeolitic imidazole framework 8, modified zif-8.

### 1. INTRODUCTION

Polymeric membrane is an emerging technology over the years with high performance separation while offering lower operating cost. It is widely applied for natural gas sweetening, oxygen enrichment, hydrogen

purification, and hydrocarbon recovery. Polymeric membrane is considered as preferable separation media to replace the conventional separation method since its separation is based on molecular size, modest energy requirement and modular equipment requirement (Baker, 2012). Polymeric membrane,

using high feed pressure as a driving force for membrane permeation, is favorable to be implemented in pressurized plant such as natural gas processing hence no additional compression needed (Baker *et al.*, 2014).

Current interest in membrane for gas separation focuses on mixed matrix membrane (MMM). MMM is a combination of polymeric material as a continuous phase and inorganic material as a dispersed phase and theoretically, their performance is superior compared to polymeric membrane. Each of MMM complements is limited by resulting new class of membrane with ease processability and high separation performance while maintaining moderate cost. For example, in CO<sub>2</sub>/CH<sub>4</sub> separation, using porous inorganic (zeolite, carbon molecular sieve) as filler would provide molecular sieving mechanism to further discriminate CH<sub>4</sub> while specific interaction with CO<sub>2</sub> provides improved surface diffusion across the membrane (Jusoh *et al.*, 2017; Rafizah *et al.*, 2008). Whereas, embedding non-porous fillers (clay particle, silica) cause tortuous permeation path that largely affects the larger gas molecule (CH<sub>4</sub>) permeation while smaller gas (CO<sub>2</sub>) is less affected (N. M. Ismail *et al.*, 2016; Surya Murali *et al.*, 2014).

Metal-organic framework (MOF) is a new class of material that has gained massive attention since its discovery. MOFs are crystalline compounds consisting of metal ions and secondary building units or organic ligands. Interesting characteristics of MOFs such as high micropore volume, large pore sizes, high phase crystallinity and high metal content offering valuable active sites are the key features of this new and emerging class of porous materials (Schlichte *et al.*, 2004). Large surface area of MOF gives advantages over other porous materials like activated carbon and zeolite has given MOF the edge in various applications such as gas storage, gas separation, catalytic application and drug delivery system. Utilizing MOF as a dispersed phase in

MMM has also provides promising results. It has been reported that the presence of organic ligand in their structure provides good interaction with the polymeric phase and subsequently minimizes interfacial defects that commonly occurred in MMM. For example, Ordoñez *et al.* (2010) has demonstrated high loading of ZIF-8, a sub-class of MOF, up to 50wt% (total solids) resulting in enormous increment in CO<sub>2</sub>/CH<sub>4</sub> selectivity with 124.89, which was almost 300% better than neat membrane (CO<sub>2</sub>/CH<sub>4</sub> selectivity = 31.49). The large increase in the membrane performance is largely related to defect-free filler-polymer interface in which the filler properties can be fully utilize to assist the separation.

In spite of attracting a lot of interest, the reports on MMM mainly focuses on density structure, which is considerably low flux to be considered as an attractive alternative to the existing technology. To minimize the transport resistance, utilizing asymmetric membrane would be beneficial. Asymmetric membrane consists of thin selective layer presence on top of porous substructure, providing minimal gas transport resistance and mechanical support (Loeb, 1981). Previous attempts on developing asymmetric MOF-class MMM in flat sheet configuration have been reported and show promising results (Nordin, Ismail, Misdan, *et al.*, 2017; Nordin, Ismail, & Yahya, 2017).

As a way forward in membrane development, hollow fiber asymmetric membrane is currently considered as the most practical approach. Compared to other configurations (i.e. flat sheet, capillary, spiral-wound), hollow fiber membrane possesses high packing density and larger effective surface area per unit module, thus resulting more productivity (CO<sub>2</sub> flux). Previously, we have successfully prepared MOF-based MMM in flat sheet configuration. Therefore, in this report, attempt to fabricate hollow fiber membrane has been made. The challenges regarding hollow fiber

MMM are highlighted using ZIF-8 as a dispersed phase. Ammonia modified ZIF-8, having higher affinity towards CO<sub>2</sub> (Md Nordin, Racha, et al., 2015), was also used to investigate different filler properties on hollow fiber MMM formation

## 2. MATERIALS AND METHODS

### 2.1. Materials

Zinc nitrate hexahydrate (Zn(NO<sub>3</sub>)<sub>2</sub>·6H<sub>2</sub>O) was purchased from Alfa Aesar. Chemicals such as 2-methylimidazole (2-MeIm), *n*-hexane, polydimethylsiloxane (PDMS) and triethylamine (TEA) were obtained from Sigma Aldrich. Polysulfone (PSf Udel® P-1700) with density of 1.24 g/cm<sup>3</sup> was procured from Solvay Plastic. Ammonium hydroxide solution (25%), *N,N*-dimethylacetamide (DMAc) tetrahydrofuran (THF) and ethanol (EtOH) were purchased from Merck. All chemicals were used without further purification.

### 2.2. ZIF-8 and Modified ZIF-8 Preparation

ZIF-8 was prepared by similar procedure described in literature (Nordin et al., 2014). Briefly, metal salt solution consist of Zn(NO<sub>3</sub>)<sub>2</sub>·6H<sub>2</sub>O (2 g, 6.72 mmol in 12.11g deionized water) while organic ligands solution consist of 2-MeIm (3.312 g, 40.34 mmol in 48.45g deionized water). TEA (3.0 mL) was added to the organic ligand solution to assist the ligand deprotonation and kept stirred for 15 minutes. The metal salt solution was added into the organic ligand solution and precipitation occurs almost instantly. After stirring for 30 minutes, the suspension was centrifuge to separate the two phases. The precipitation was washed with deionized water for three times to remove excess reactant before dried at 60°C for 12 hours. The powdered sample is collected and denoted as virgin ZIF-8.

The virgin ZIF-8 was then modified following similar procedure reported in our previous work (Md Nordin, Racha, et al., 2015). Firstly, 1.0 g of the virgin ZIF-8 was added into 10 mL deionized water and sonicated to ensure the suspension is uniformly dispersed. Ammonium hydroxide solution (25 mL) was added to the suspension and continues sonication before being vigorously stirred for 24 h at 60°C. The sample was collected via centrifugation and washed with deionized water (3 times) before being dried in an oven (60°C) overnight. The powdered sample is collected and denoted as modified ZIF-8.

### 2.3. Membrane Solution Preparation

Membrane formulation used in this study is adapted from literatures (Bhardwaj et al., 2003; Gordeyev et al., 2001; Ismail et al., 1999; Magueijo et al., 2013; Wahab et al., 2012) with 22wt% of PSf, 31.8wt% of DMAc (non-volatile solvent), 31.8wt% of THF (volatile solvent), and 14.4wt% of EtOH (non-solvent). Briefly, 0.5wt% (total solids) of virgin or modified ZIF-8 was dispersed into DMAc/THF solvent and sonicated to breaks the bulk particles. The dispersed ZIF-8 solution was then vigorously stirred before approximately 10% of polymer was added under stirring for the priming purpose. Remaining polymer was gradually added and the mixture was kept stirred until the solution became homogeneous. The ethanol was added drop-wise to avoid solidification of membrane solution. The solution was kept stirred until homogeneous and sonicated prior to spinning process. Similar procedure was used for neat hollow fiber membrane with exclusion of filler incorporation.

### 2.4. Hollow Fiber Membrane Preparation

The hollow fiber membranes were prepared using custom made spinning process and illustrated in **Figure 1** with parameters tabulated in **Table 1**. Briefly, membrane solution placed in the solution reservoir was extruded

from spinneret undergoes dry/wet phase inversion. Forced convection (acrylic chamber) was done using different N<sub>2</sub> flowrate and different air gap length for dry inversion. Different spinning parameters were employed to identify the optimized spinning conditions on each formulation. The membrane undergoes wet inversion in coagulation bath before the samples were collected. After spinning, the membranes were left in water bath for 12 hours to further remove trapped solvent. Membrane post-treatment was done by immersing in ethanol (2 hours) and n-hexane (2 hours) before left for drying at room temperature for 12 hours. The surface of the membrane was then brought into contact with 3wt% PDMS/n-

hexane solution for 10 min to seal possible pinholes before they were “cured” at 60°C overnight.

It should be noted that air gap used in this study was only at 20 cm and 30 cm. Air gap lower than 20 cm had less dry inversion time would resulting poor membrane performance. Whereas, at higher air gap, we experienced fiber “swing” after extruded from spinneret and hit force convection chamber. Similarly, higher force convection flowrate agitate the extruded fiber and hit the convection chamber. Thus, fiber spun at higher air gap (>30 cm) and higher FC (>10 L/min) is not presented.

**Table 1.** Hollow fiber preparation parameters

Materials	Composition (wt%)
Polysulfone (PSf Udel® P-1700)	22
Dimethylacetamide (DMAc)	31.8
Tetrahydrofurane (THF)	31.8
Ethanol (EtOH)	14.4
Filler (wt% from total solids)	0.5
Spinning parameter	Condition
Spinneret dimension (OD/ID)	0.6/0.3 mm
Bore fluid flowrate	0.83 mL/min
Air gap distance	20, 30 cm
Force convection (N <sub>2</sub> ) flowrate	4, 7, and 10 L/min
Dope extrusion rate	2.5 mL/min
Coagulation bath	Water
Bore fluid media	20wt% Potassium acetate aqueous solution

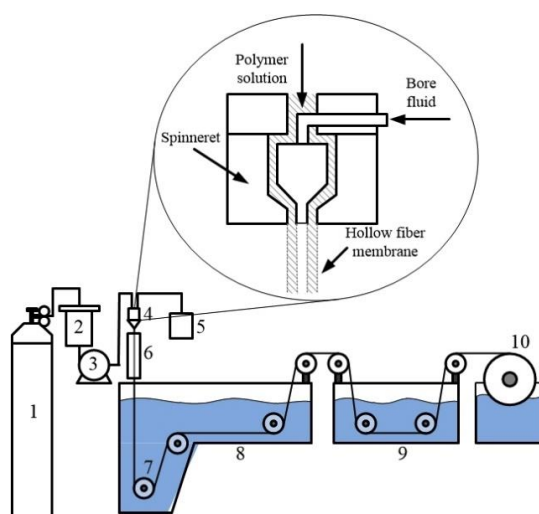


**Figure 1.** Schematic diagram of the spinning system: (1) N<sub>2</sub> tank, (2) Dope solution reservoir, (3) gear pump, (4) spinneret, (5) Bore fluid solution, (6) force convection chamber, (7) roller, (8) coagulation bath, (9) washing bath, and (10) collection drum

## 2.5. Characterization

Attenuated total reflectance infrared spectroscopy (ATR-IR) analysis was conducted using a Perkin Elmer UATR (Single Reflection Diamond) for Spectrum Two to observe the functional groups of virgin and modified ZIF-8s.

XRD analysis was used to confirm that the phase of the ZIF-8 was similar to that reported in the literature and to monitor the changes in ZIF-8 crystallinity after modification. X-Ray Diffraction (XRD) analysis using a Siemens D5000 Diffractometer is non-destructive analysis to identify the structure of the sample by measuring  $2\theta$  angles. The XRD will emit X-rays towards the sample and the X-rays are diffracted at different angles and intensities by  $\text{CuK}\alpha$  radiation with a wavelength ( $\lambda$ ) = 1.54 Å at room temperature.

The specific surface area and pore volume of the virgin ZIF-8 and modified ZIF-8 crystals were measured using a Micromeritics gas adsorption analyzer ASAP2010 instrument equipped with commercial software for calculation and analysis. The BET surface area was calculated from the adsorption isotherms using the standard Brunauer–Emmett–Teller (BET) equation. The total pore volume was evaluated by converting the adsorption amount at  $p/p_0 = 0.95$  to a volume of liquid adsorbate. The mesopore volume was obtained using a BJH plot while the micropore volume was obtained using the t-plot method of Lippens and de Boer with the adsorption data.

A transmission electron microscope (TEM) (JEOL, JSM-6701FJEOL 1230) was applied to observe the macrostructures of the ZIF-8. Samples were prepared by dispersing ZIF-8 powder in methanol. A drop of methanol was used for the dispersion of ZIF-8 on carbon-coated copper grids operating at 300 kV.

FESEM was used to observe morphology of membrane under high magnification using Hitachi su8020 JEOL JSM-7600F. Membranes sample were fractured under cryogenic condition in liquid nitrogen to avoid sample flattening. Then, the fractured sample was sputter coated with gold to create conductive layer on sample surface before tested.

## 2.6. Gas Permeation Test

Gas permeation tests were performed using a constant pressure variable volume system described elsewhere (A. F. Ismail *et al.*, 2003). Membrane modules consist of five hollow fiber were potted before placed in permeation cell. The permeation cell was then exposed to pure  $\text{CH}_4$  and  $\text{CO}_2$  gas, respectively, at 4 bar and temperature of  $27^\circ\text{C}$ . Pressure-normalized flux (permeance) of gas  $i$  was calculated as follows:

$$\left(\frac{P_i}{l}\right) = \frac{1}{A\Delta p} \times \frac{dV_i}{dt} \quad (1)$$

where  $i$  represents the gas penetrant,  $V_i$  is the volume of gas permeated through the membrane ( $\text{cm}^3$ , STP),  $A$  is the effective membrane area ( $\text{cm}^2$ ),  $t$  the permeation time (s) and  $\Delta p$  is the transmembrane pressure drop ( $\text{cmHg}$ ). Permeance is expressed in gas permeation units, GPU, as

$$1 \text{ GPU} = 1 \times 10^{-6} \text{ cm}^3 (\text{STP}) \text{ cm}^{-2} \text{ s}^{-1} \text{ cmHg}^{-1}.$$

Selectivity was obtained using Eq. (3):

$$\alpha_{i/j} = \frac{(P_i/l)}{(P_j/l)} \quad (2)$$

where  $\alpha_{i/j}$  is the selectivity of gas penetrant  $i$  over gas penetrant  $j$ ,  $P_{i/l}$  and  $P_{j/l}$  are the permeance of gas penetrant  $i$  and  $j$ , respectively.

### 3. RESULTS AND DISCUSSION

#### 3.1. Filler Characterizations

The prepared fillers were characterized by XRD to identify their phase crystallinity (Figure 2a). Both virgin and modified ZIF-8 shows the presents of peak at  $2\theta = 7.30, 10.35, 12.70, 14.80, 16.40$  and  $18.00^\circ$  correspond to planes (110), (200), (211), (220), (310), and (222), respectively. Slight peak intensification was also observed after modification indicates the crystallinity of ZIF-8 increased after modification. This is likely due to further removal of guest molecules within the ZIF-8 pores during modification that commonly cause destructive interference of the XRD pattern (Perez et al., 2009). Additional peak was observed for modified ZIF-8 at  $2\theta = 10.96^\circ$  presumably due to cage reordering on the cavity of ZIF-8 (Bae et al., 2009; Schröder et al., 2008). The TEM analysis of virgin ZIF-8 shows rhombic dodecahedron structure with particle size estimated around 133 nm (Figure 2i). The particle size of modified ZIF-8 is assumed to similar with the virgin ZIF-8 since no apparent difference between the peak widths of the XRD pattern, which correlate with their crystal size.

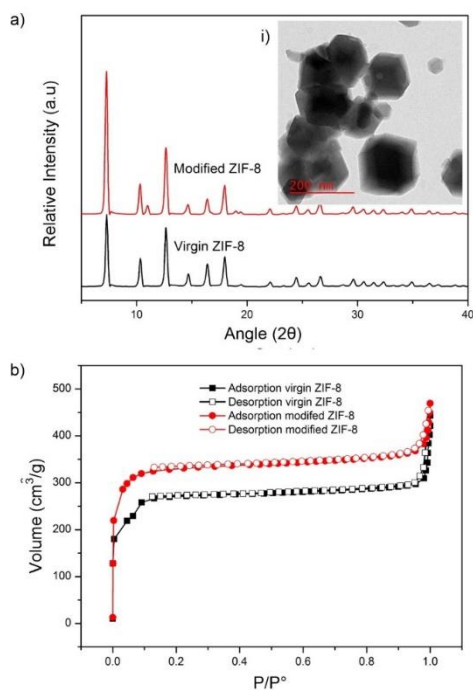


**Figure 2.** Properties of virgin and modified ZIF-8 with a) x-ray diffraction, i) morphology of virgin ZIF-8, and b)  $N_2$  sorption isotherm

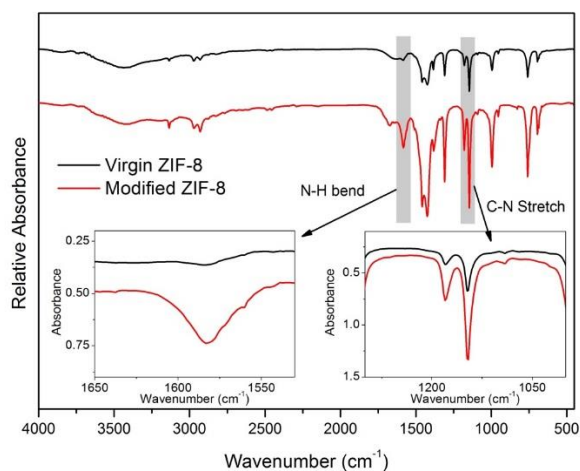


**Figure 3.** The IR-spectra of virgin and modified ZIF-8

The  $N_2$  sorption isotherm of both samples shows type-I isotherm which reflects to permanent microporosity with no hysteresis loop of the samples (Figure 2b). At relatively low pressure ( $p/p_0 < 0.1$ ), steep increase reveals the microporosity while steep increase at high pressure ( $p/p_0 > 0.9$ ) indicates the textural meso/macroporosity of the crystal (Md Nordin, Ismail, et al., 2015). The virgin ZIF-8 possess BET surface area of  $1031.3 \text{ m}^2/\text{g}$  with total pore volume of  $0.5422 \text{ cm}^3/\text{g}$ . After modification, the BET surface area increased to  $1250.5 \text{ m}^2/\text{g}$  with total pore volume of  $0.5803 \text{ cm}^3/\text{g}$ . These results further confirm that removal of guest molecule after modification improves their textural properties.

The IR-spectra of ZIF-8 prior and after modification are presented in Figure 3. The absorption bands between  $3135$  and  $2929 \text{ cm}^{-1}$  can be attributed to the aromatic and the aliphatic C-H stretching of methylimidazole, respectively, peak at  $1584 \text{ cm}^{-1}$  was due to the C=N stretching mode, whereas bands between  $1350$ – $1500 \text{ cm}^{-1}$  can be assigned to the entire ring stretching. Overall, the IR spectra are in good agreement with other studies (Park et al., 2006; Zhang et al., 2011). After

modification, it was observed that the intensification of peak at 1250–1020 cm<sup>-1</sup> represent the aliphatic C–N stretch, and at 1650–1580 cm<sup>-1</sup> represent the N–H bend. Hence, the results suggested that ZIF-8 has successfully undergoes modification.

### 3.2. Hollow Fiber Membrane Performances

The performances of the prepared membranes are illustrated in **Figure 4**, with different air gap distance and FC. It was observed that increasing FC rate resulting poor CO<sub>2</sub> permeance and CO<sub>2</sub>/CH<sub>4</sub> selectivity (**Figure 4a**). For example, at AG = 30 cm, the CO<sub>2</sub> permeance and CO<sub>2</sub>/CH<sub>4</sub> selectivity of prepared the membrane diminished from 104.38 GPU and 29.28 to 57.65 GPU and 12.13, respectively, after FC was increased from 4 to 10 L/min. As FC rate increase, THF evacuate from the spun fiber progressively and cause thicker membrane skin layer, providing higher mass transfer resistance and leads to diminished CO<sub>2</sub> permeance. Thicker selective layer would provide either similar or higher gas pair selectivity. However, it was observed that CO<sub>2</sub>/CH<sub>4</sub> selectivity was diminished as FC increased, indicating severe defects on the selective layer of the resulted membranes.

**Table 2** shows the ideal CO<sub>2</sub> separation properties of hollow fiber membranes spun at 30 cm air gap with FC of 4 L/min. In our previous reports, incorporating both virgin and modified ZIF-8s into PSf matrix are beneficial towards improving membrane performances (Md Nordin, Ismail, *et al.*, 2015; Md Nordin, Racha, *et al.*, 2015). Contradictory with the behavior in flat sheet membrane, incorporating of 0.5wt% (total solids) of either virgin or modified ZIF-8 somehow deteriorate the membrane performance. The drop for PSf/virgin ZIF-8 was approximately 60% for both CO<sub>2</sub> permeance and CO<sub>2</sub>/CH<sub>4</sub> selectivity, while PSf/modified ZIF-8 suffered 28% drop in

CO<sub>2</sub> permeance and 52% in CO<sub>2</sub>/CH<sub>4</sub> selectivity.

Both fillers incorporated have high affinity with CO<sub>2</sub> and highly porous, especially modified ZIF-8, which boost the membrane performances. These unforeseen deteriorations are likely originated from membrane solution stability after ZIF-8s incorporation. The membrane solution stability altered after filler incorporation could cause different solvent-nonsolvent exchange rate and disrupt membrane formation. **Figure 5** show cross sectional morphology of hollow fiber neat PSf, PSf/virgin ZIF-8, and PSf/modified ZIF-8 spun under similar spinning parameters. It was observed that neat PSf membrane possess large teardrop morphology (**Figure 5a,ii**) resulted from indicators of rapid solvent-nonsolvent demixing rates. Whereas, both MMMs show smaller teardrop morphology, suggesting the presence of ZIF-8 (either virgin or modified) cause slower demixing rate.

**Table 2.** Comparison between neat PSf, PSf/virgin ZIF-8 and PSf/modified ZIF-8 hollow fiber membrane at pressure 4 bar

Sample*	Ideal CO <sub>2</sub> separation	
	CO <sub>2</sub> Permeance (GPU) <sup>a</sup>	CO <sub>2</sub> /CH <sub>4</sub> selectivity <sup>b</sup>
PSf	104.39 ± 15.76	29.28 ± 5.87
PSf/virgin ZIF-8	42.02 ± 0.49	11.52 ± 0.94
PSf/modified ZIF-8	74.71 ± 1.94	14.17 ± 0.63

\* Hollow fiber spun at 30 cm air gap, using 4 L/min forced convection

<sup>a</sup> GPU = 1 × 10<sup>-6</sup> cm<sup>3</sup> cm<sup>-2</sup> s<sup>-1</sup> cmHg<sup>-1</sup>

<sup>b</sup> The ideal selectivity presented is based on average of membrane modules tested, and not necessary equal to the ratio of average permeance

± Represent the standard deviation

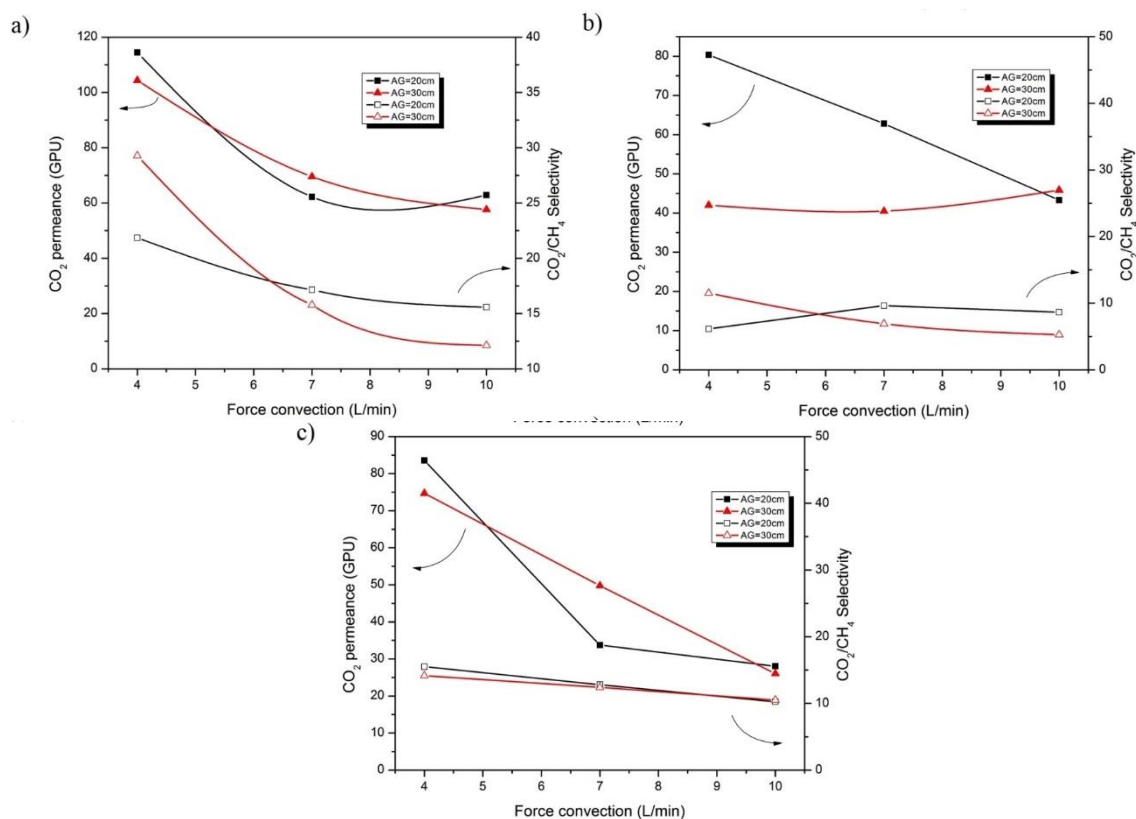


**Figure 4.** The CO<sub>2</sub> permeance (GPU) (closed symbols) and CO<sub>2</sub>/CH<sub>4</sub> selectivity (open symbols) of (a) neat, (b) PSf/virgin ZIF-8, and (c) PSf/modified ZIF-8 hollow fiber membrane produced using different air gap (black line represent AG = 20 cm, red line represent AG = 30 cm) and force convection flowrate

The solvent demixing rate in this study was more prominent compared to reports in our previous works (Md Nordin, Ismail, *et al.*, 2015; Md Nordin, Racha, *et al.*, 2015). This is likely due to the different solvents used; where *N*-methyl-2-pyrrolidone (NMP) was used as solvent in the literature, while DMAc was used as solvent in this study. Utilizing appropriate solvent is crucial in MMM development. Mahajan and Koros (2000) emphasize that an ideal MMM solution system requires polymer-filler interaction stronger than filler-solvent and polymer solvent, hence solvent can be easily desorb by the filler and minimize stress on filler's surface. Compared to DMAc, NMP has higher Hansen solubility parameter for PSf and can easily dissolve the polymer (Pourafshari Chenar *et al.*, 2013). However,

there is limitation in literature study regarding liquid-solid interaction strength parameters available for ZIF-8 in solvent and conclusive statement cannot be made. Judging from different trends of PSf/ZIF performance using NMP and DMAc as solvent, it can be postulated that ZIF-8 are hardly desorb DMAc compared to NMP and promotes PSf to rigidified surrounding the filler. This causes ZIF-8 pores to be unavailable due to severe pore blockage by rigidification for penetrant, causing poor CO<sub>2</sub> permeance and CO<sub>2</sub>/CH<sub>4</sub> selectivity simultaneously. The PSf/modified ZIF-8 is superior compared to PSf/virgin ZIF-8 due to higher affinity of modified ZIF-8 towards CO<sub>2</sub> (Md Nordin, Racha, *et al.*, 2015); however, they are still underperformed when compared to neat PSf membrane.



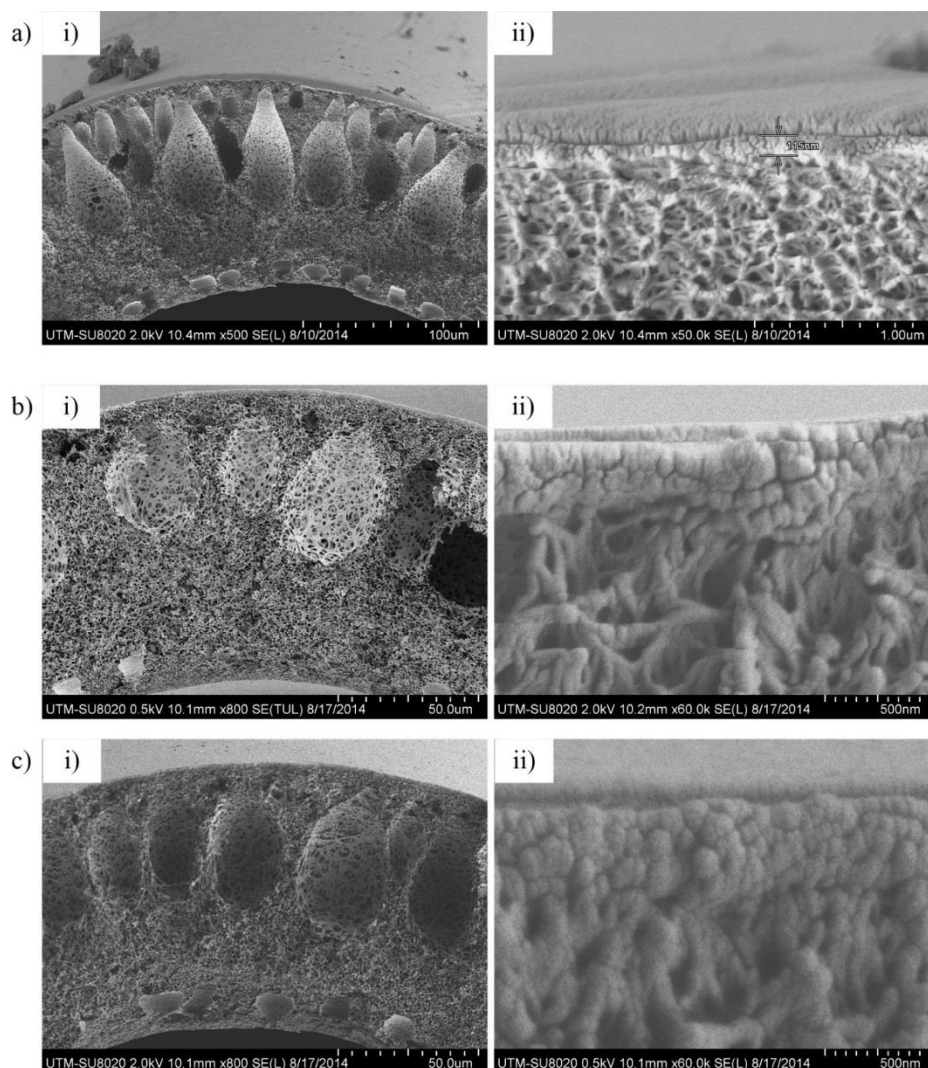


**Figure 5.** Cross sectional morphology of (a) neat PSf, (b) PSf/virgin ZIF-8, and (c) PSf/modified ZIF-8 hollow fiber membrane (AG = 30 cm, FC = 4 L/min) with different magnification

#### 4. CONCLUSION

Development of hollow fiber membrane is more favorable for industrial applications compared to flat sheet membranes mainly due to high module packing per unit area, thus providing higher productivity in single membrane unit is inevitable. The prepared hollow fiber membrane has shown good separation properties with CO<sub>2</sub> permeance of 104.39 GPU and CO<sub>2</sub>/CH<sub>4</sub> selectivity of 29.28. Incorporating fillers (either virgin or modified ZIF-8) somehow shows discouraging results, where severe deterioration in both CO<sub>2</sub>

permeance and CO<sub>2</sub>/CH<sub>4</sub> selectivity were observed despite literatures suggest positive remarks. This phenomenon is likely generated from membrane solution stability changes after ZIF-8s incorporated and compatibility of ZIF-8 with DMAc as solvent. Hence, scrutinized studies regarding hollow fiber configuration such as spinning parameters (dope extrusion rate, bore fluid flowrate, collection speed, coagulation bath temperature) and MMM solution stability (ternary diagram, solution viscosity, filler

dispersity in solvent) are necessary to develop high performance hollow fiber MMM.

## 5. ACKNOWLEDGEMENTS

The authors gratefully acknowledge the Post-Doctoral Fellowship Scheme for the project "Development of Metal-Organic Framework/Graphene Oxide (MOF/GO) Composite Mixed Matrix Membrane for Gas Separation"

under Universiti Teknologi Malaysia with the grant number PY/2015/05319.

## 6. AUTHORS' NOTE

The author(s) declare(s) that there is no conflict of interest regarding the publication of this article. Authors confirmed that the data and the paper are free of plagiarism.

## 7. REFERENCES

- Bae, Y.-S., Farha, O. K., Hupp, J. T., & Snurr, R. Q. (2009). Enhancement of CO<sub>2</sub>/N<sub>2</sub> selectivity in a metal-organic framework by cavity modification. *Journal of Materials Chemistry*, 19(15), 2131. doi:10.1039/b900390h
- Baker, R. W. (2012). *Gas Separation Membrane Technology and Applications*: Wiley.
- Baker, R. W., & Low, B. T. (2014). Gas Separation Membrane Materials: A Perspective. *Macromolecules*, 47(20), 6999-7013. doi:10.1021/ma501488s
- Bhardwaj, V., Macintosh, A., Sharpe, I. D., Gordeyev, S. A., & Shilton, S. J. (2003). Polysulfone Hollow Fiber Gas Separation Membranes Filled with Submicron Particles. *Annals of the New York Academy of Sciences*, 984(1), 318-328. doi:10.1111/j.1749-6632.2003.tb06009.x
- Gordeyev, S. A., Lees, G. B., Dunkin, I. R., & Shilton, S. J. (2001). Super-selective polysulfone hollow fiber membranes for gas separation: rheological assessment of the spinning solution. *Polymer*, 42(9), 4347-4352. doi:http://dx.doi.org/10.1016/S0032-3861(00)00787-4
- Ismail, A. F., Dunkin, I. R., Gallivan, S. L., & Shilton, S. J. (1999). Production of super selective polysulfone hollow fiber membranes for gas separation. *Polymer*, 40(23), 6499-6506. doi:http://dx.doi.org/10.1016/S0032-3861(98)00862-3
- Ismail, A. F., & Lai, P. Y. (2003). Effects of phase inversion and rheological factors on formation of defect-free and ultrathin-skinned asymmetric polysulfone membranes for gas separation. *Separation and Purification Technology*, 33(2), 127-143. doi:10.1016/s1383-5866(02)00201-0
- Ismail, N. M., Ismail, A. F., Mustafa, A., Zulhairun, A. K., & Nordin, N. A. H. M. (2016). Enhanced carbon dioxide separation by polyethersulfone (PES) mixed matrix membranes deposited with clay *Journal of Polymer Engineering* (Vol. 36, pp. 65).
- Jusoh, N., Yeong, Y. F., Lau, K. K., & M. Shariff, A. (2017). Enhanced gas separation performance using mixed matrix membranes containing zeolite T and 6FDA-durene polyimide. *Journal of Membrane Science*, 525, 175-186. doi:https://doi.org/10.1016/j.memsci.2016.10.044
- Loeb, S. (1981). The Loeb-Sourirajan Membrane: How It Came About *Synthetic Membranes*: (Vol. 153, pp. 1-9): AMERICAN CHEMICAL SOCIETY.

- Magueijo, V. M., Anderson, L. G., Fletcher, A. J., & Shilton, S. J. (2013). Polysulfone mixed matrix gas separation hollow fibre membranes filled with polymer and carbon xerogels. *Chemical Engineering Science*, 92, 13-20. doi:10.1016/j.ces.2013.01.043
- Mahajan, R., & Koros, W. J. (2000). Factors Controlling Successful Formation of Mixed-Matrix Gas Separation Materials. *Industrial & Engineering Chemistry Research*, 39(8), 2692-2696. doi:10.1021/ie990799r
- Md Nordin, N. A. H., Ismail, A. F., Mustafa, A., Murali, R. S., & Matsuura, T. (2015). Utilizing low ZIF-8 loading for an asymmetric PSf/ZIF-8 mixed matrix membrane for CO<sub>2</sub>/CH<sub>4</sub> separation. *RSC Advances*, 5(38), 30206-30215. doi:10.1039/c5ra00567a
- Md Nordin, N. A. H., Racha, S. M., Matsuura, T., Misdan, N., Abdullah Sani, N. A., Ismail, A. F., & Mustafa, A. (2015). Facile modification of ZIF-8 mixed matrix membrane for CO<sub>2</sub>/CH<sub>4</sub> separation: synthesis and preparation. *RSC Advances*, 5(54), 43110-43120. doi:10.1039/c5ra02230d
- Nordin, N. A. H. M., Ismail, A. F., Misdan, N., & Nazri, N. A. M. (2017). Modified ZIF-8 mixed matrix membrane for CO<sub>2</sub>/CH<sub>4</sub> separation. *AIP Conference Proceedings*, 1891(1), 020091. doi:10.1063/1.5005424
- Nordin, N. A. H. M., Ismail, A. F., Mustafa, A., Goh, P. S., Rana, D., & Matsuura, T. (2014). Aqueous room temperature synthesis of zeolitic imidazole framework 8 (ZIF-8) with various concentrations of triethylamine. *RSC Advances*, 4(63), 33292-33300. doi:10.1039/C4RA03593C
- Nordin, N. A. H. M., Ismail, A. F., & Yahya, N. (2017). Zeolitic imidazole framework 8 decorated graphene oxide (ZIF-8/GO) mixed matrix membrane (MMM) for CO<sub>2</sub>/CH<sub>4</sub> separation. *Jurnal Teknologi*, 79(1-2), 59-63. Retrieved from <https://www.scopus.com/inward/record.uri?eid=2-s2.0-85011632571&partnerID=40&md5=abc2b199d85079c7451c88a02db7afdb>
- Ordoñez, M. J. C., Balkus, K. J., Ferraris, J. P., & Musselman, I. H. (2010). Molecular sieving realized with ZIF-8/Matrimid® mixed-matrix membranes. *Journal of Membrane Science*, 361(1), 28-37. doi:https://doi.org/10.1016/j.memsci.2010.06.017
- Park, K. S., Ni, Z., Cote, A. P., Choi, J. Y., Huang, R., Uribe-Romo, F. J., . . . Yaghi, O. M. (2006). Exceptional chemical and thermal stability of zeolitic imidazolate frameworks. *Proc Natl Acad Sci U S A*, 103(27), 10186-10191. doi:10.1073/pnas.0602439103
- Perez, E. V., Balkus, K. J., Ferraris, J. P., & Musselman, I. H. (2009). Mixed-matrix membranes containing MOF-5 for gas separations. *Journal of Membrane Science*, 328(1-2), 165-173. doi:10.1016/j.memsci.2008.12.006
- Pourafshari Chenar, M., Rajabi, H., Pakizeh, M., Sadeghi, M., & Bolverdi, A. (2013). Effect of solvent type on the morphology and gas permeation properties of polysulfone-silica nanocomposite membranes. *Journal of Polymer Research*, 20(8), 1-9. doi:10.1007/s10965-013-0216-3
- Rafizah, W. A. W., & Ismail, A. F. (2008). Effect of carbon molecular sieve sizing with poly(vinyl pyrrolidone) K-15 on carbon molecular sieve-polysulfone mixed matrix membrane.

*Journal of Membrane Science*, 307(1), 53-61. doi:<https://doi.org/10.1016/j.memsci.2007.09.007>

Schlichte, K., Kratzke, T., & Kaskel, S. (2004). Improved synthesis, thermal stability and catalytic properties of the metal-organic framework compound  $\text{Cu}_3(\text{BTC})_2$ . *Microporous and Mesoporous Materials*, 73(1-2), 81-88. doi:10.1016/j.micromeso.2003.12.027

Schröder, F., Esken, D., Cokoja, M., van den Berg, M. W. E., Lebedev, O. I., Van Tendeloo, G., . . . Fischer, R. A. (2008). Ruthenium Nanoparticles inside Porous  $[\text{Zn}_4\text{O}(\text{bdc})_3]$  by Hydrogenolysis of Adsorbed  $[\text{Ru}(\text{cod})(\text{cot})]$ : A Solid-State Reference System for Surfactant-Stabilized Ruthenium Colloids. *J Am Chem Soc*, 130(19), 6119-6130. doi:10.1021/ja078231u

Surya Murali, R., Praveen Kumar, K., Ismail, A. F., & Sridhar, S. (2014). Nanosilica and H-Mordenite incorporated Poly(ether-block-amide)-1657 membranes for gaseous separations. *Microporous and Mesoporous Materials*, 197, 291-298. doi:<https://doi.org/10.1016/j.micromeso.2014.07.001>

Wahab, M. F. A., Ismail, A. F., & Shilton, S. J. (2012). Studies on gas permeation performance of asymmetric polysulfone hollow fiber mixed matrix membranes using nanosized fumed silica as fillers. *Separation and Purification Technology*, 86, 41-48. doi:10.1016/j.seppur.2011.10.018

Zhang, Z., Xian, S., Xi, H., Wang, H., & Li, Z. (2011). Improvement of  $\text{CO}_2$  adsorption on ZIF-8 crystals modified by enhancing basicity of surface. *Chemical Engineering Science*, 66(20), 4878-4888. doi:10.1016/j.ces.2011.06.051

Zimmerman, C. M., Singh, A., & Koros, W. J. (1997). Tailoring mixed matrix composite membranes for gas separations. *Journal of Membrane Science*, 137(1), 145-154. doi:[https://doi.org/10.1016/S0376-7388\(97\)00194-4](https://doi.org/10.1016/S0376-7388(97)00194-4)